Initial-state Interactions in Drell-Yan Processes at Hadronic Collisions

Dae Sung Hwang

Sejong University

EDS'09
CERN, June 29 - July 3, 2009

Contents

Λ **Polarization (SSA)**

$p + p^{\uparrow} \longrightarrow \pi^0 + X$ **at STAR (SSA)**

SSA in Semi-Inclusive DIS

Final and Initial State Interactions

Drell-Yan Processes

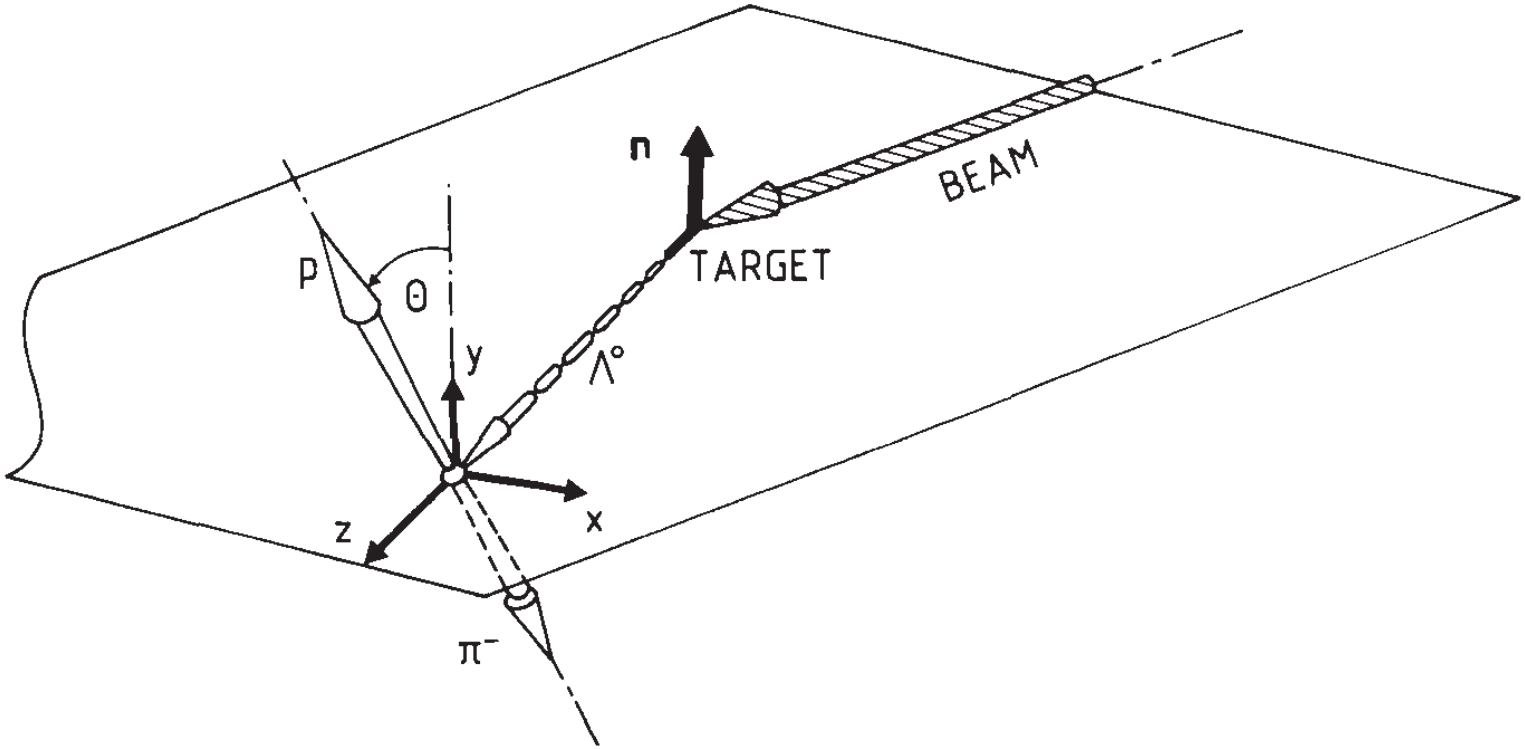

Fig. 9. Momentum vector diagram of Λ^0 decay. The y-axis is perpendicular to the scattering plane.

Experimental method for measuring the polarization of Λ^0.

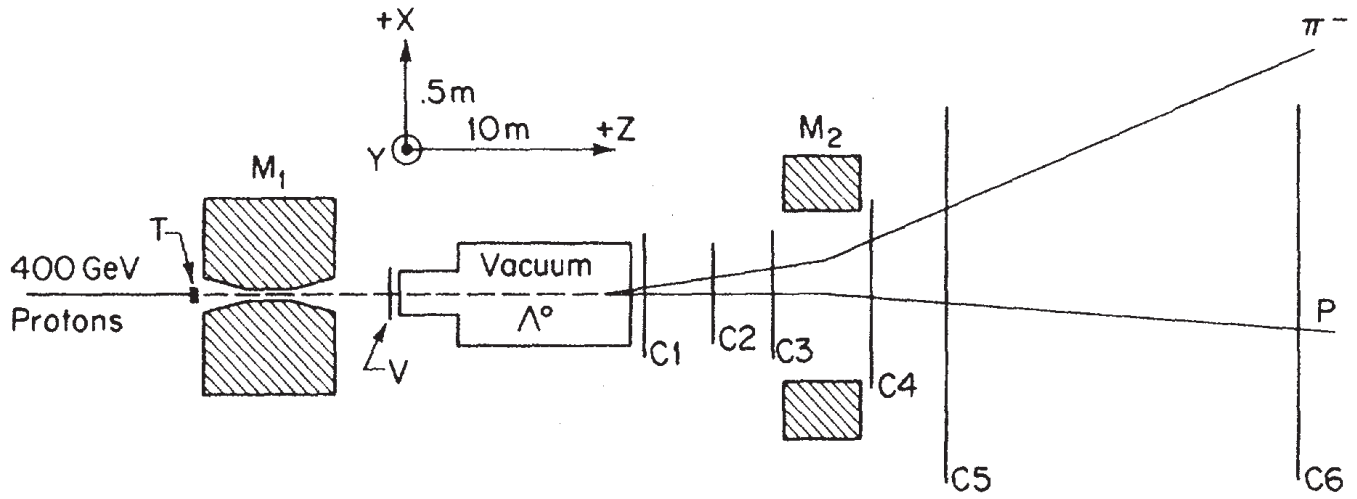

FIG. 1. Plan view of the neutral hyperon beam and spectrometer. The production angle was in the y-z plane and is not shown in this view. The elements are described in the text. The electronic trigger required no signal from the veto counter, V, and one hit in each chamber, C_i, except C_5 in which two hits one on each side of the neutral beamline were required. A typical $\Lambda^0 \to p\pi^-$ decay is shown.

400 GeV $p + Be \to \Lambda^0(\overline{\Lambda}^0) + X$ Fermilab. 1978.

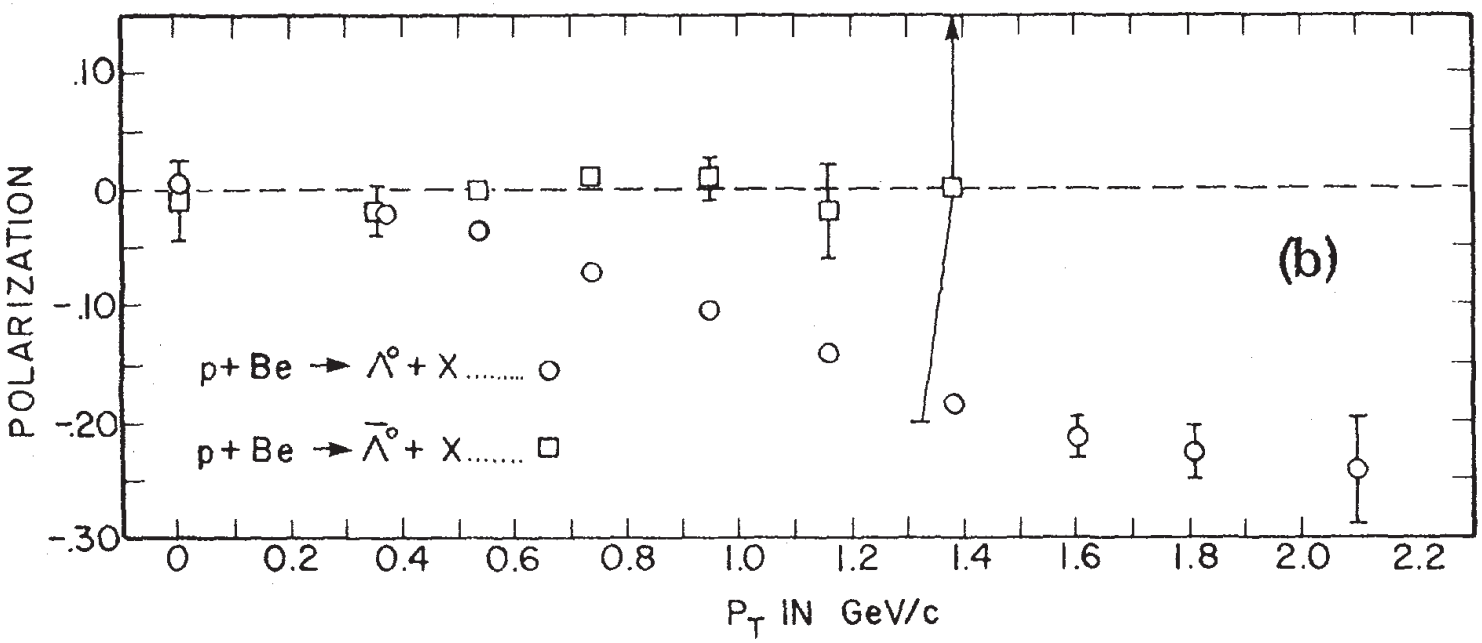

FIG. 3. (a) Λ^0 polarization from this experiment compared to that from 300-GeV incident protons from Ref. 1 as a function of p_T. The number in parentheses is the average value of x for that point. (b) Λ^0 and $\overline{\Lambda}^0$ polarization from this experiment. The polarization is defined as positive along $\hat{n} = (\vec{k}_p \times \vec{k}_\Lambda)/|\vec{k}_p \times \vec{k}_\Lambda|$.

400 GeV $p + Be \rightarrow \Lambda^0(\overline{\Lambda}^0) + X$ Fermilab. 1978.

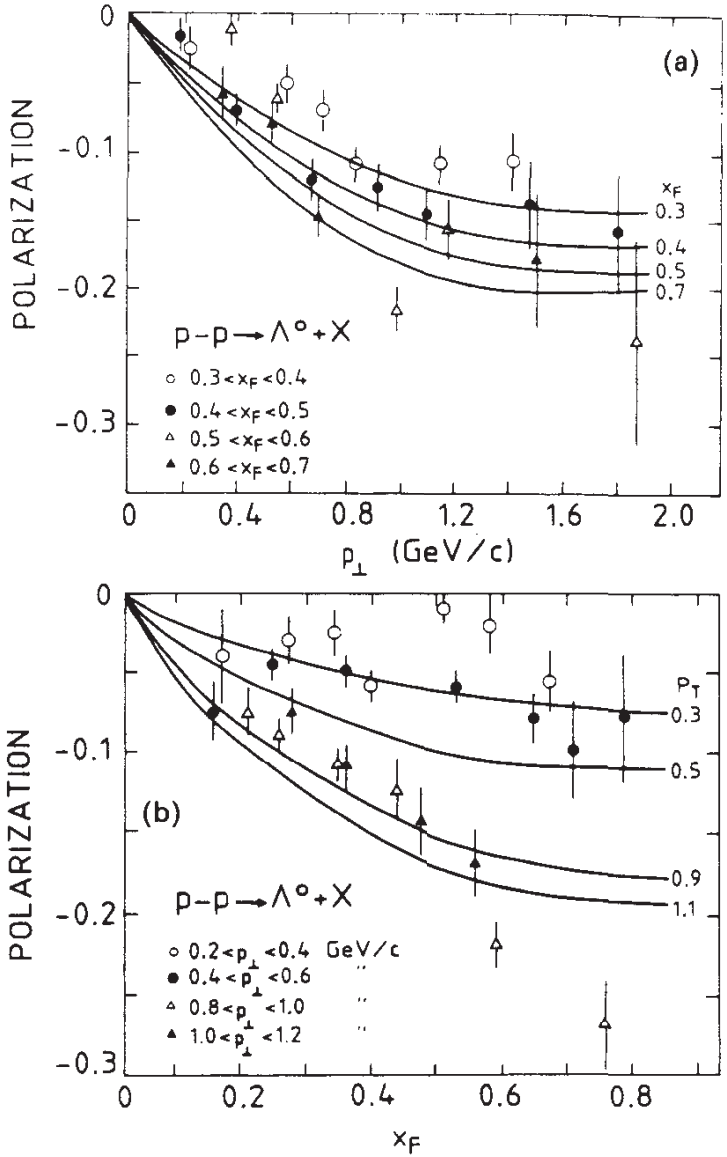

Fig. 39. Comparison of the DeGrand–Miettinen model predictions for the Λ^0 polarization with data from the inclusive p–p interaction at 400 GeV: a) fixed x_F, b) fixed $p_\perp$.

400 GeV $p + p \to \Lambda^0(\overline{\Lambda}^0) + X$ Fermilab. 1980.

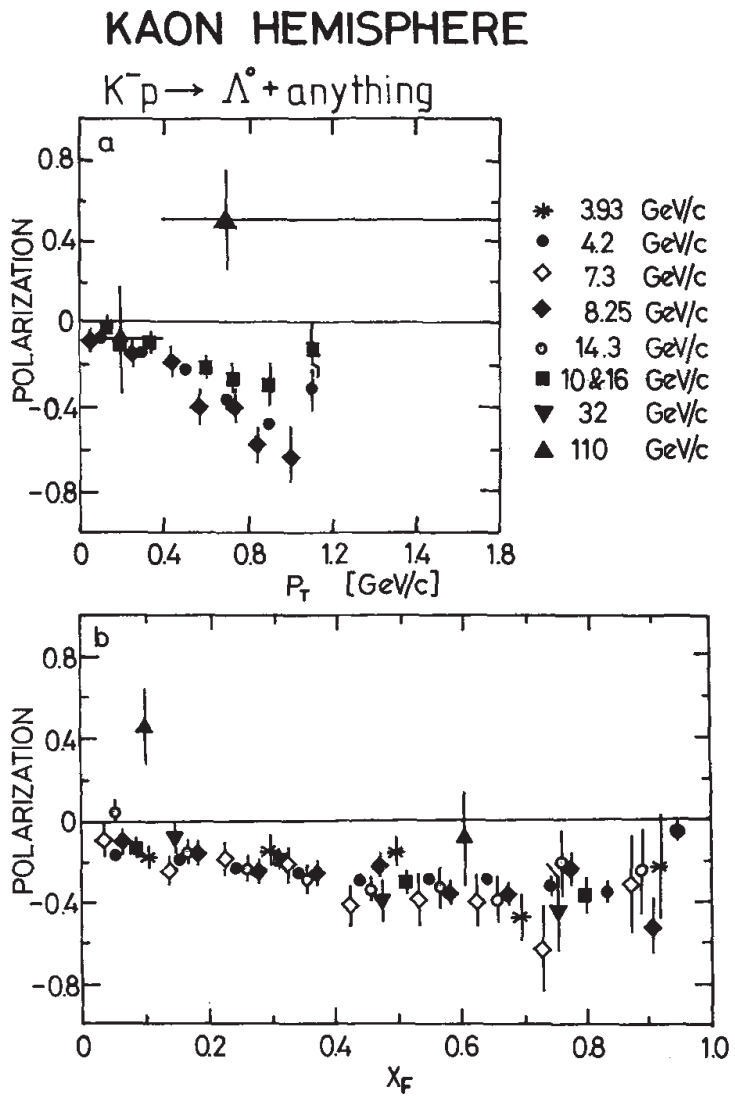

Fig. 4a and b. Polarization of Λ^0 produced in the K^- hemisphere as a function of p_t **a** and x_F **b**

110 GeV $K^+ - p \to \Lambda^0 + X$ CERN SPS 1985.

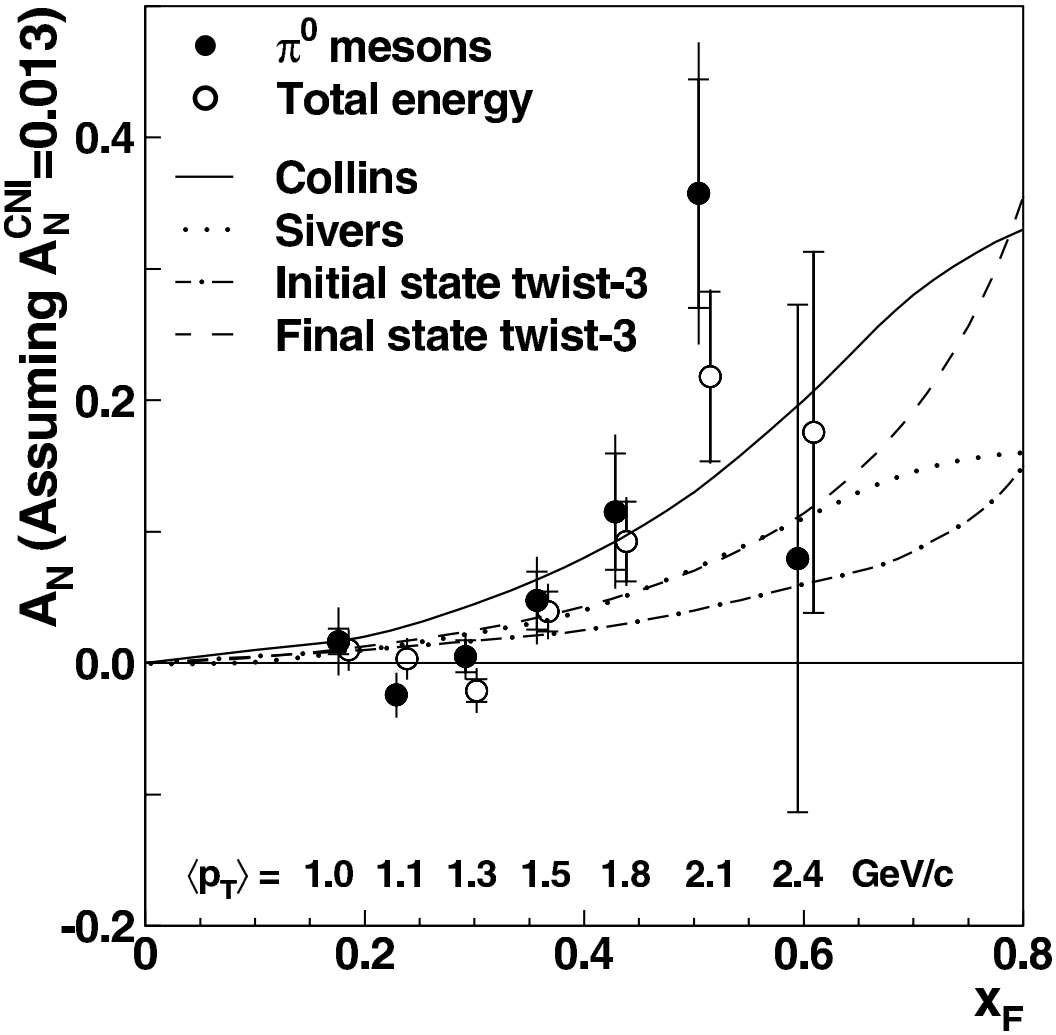

$\sqrt{s} = 200$ GeV $p + p^{\uparrow} \rightarrow \pi^0 + X$ at STAR (RHIC) 2004.

$e^- e^+ \longrightarrow p\overline{p}$

$$\langle pp'|J^\mu(0)|0\rangle = \overline{u}(P)\left[F_1(q^2)\gamma^\mu + F_2(q^2)\frac{i}{2M}\sigma^{\mu\alpha}q_\alpha\right]v(P')\ .$$

$$G_E(q^2) = F_1(q^2) + \frac{q^2}{4m^2}F_2(q^2)\ , \qquad G_M(q^2) = F_1(q^2) + F_2(q^2)\ .$$

Differential cross section is given by

$$\begin{aligned}\frac{d\sigma}{d\cos\theta} &= \frac{\pi\alpha^2\sqrt{1-\frac{4M^2}{q^2}}}{2q^2} \\ &\times \left[\ |G_M(q^2)|^2(1+\cos^2\theta) \ + \ \frac{4M^2}{q^2}|G_E(q^2)|^2\sin^2\theta \right. \\ &\left. - \ (\vec{s}\cdot\hat{y})\ \frac{2M}{\sqrt{q^2}}\ \sin 2\theta\ \mathrm{Im}[G_M^* G_E]\ \right]\ ,\end{aligned}$$

where $\hat{y} = (\hat{k}\times\hat{p})/|\hat{k}\times\hat{p}|$.

From the above equation the single-spin asymmetry is given by

$$\mathcal{P}_y = \frac{-\frac{2M}{\sqrt{q^2}}\,\sin 2\theta\,\mathrm{Im}[G_M^* G_E]}{|G_M(q^2)|^2(1+\cos^2\theta)+\frac{4M^2}{q^2}|G_E(q^2)|^2\sin^2\theta}\ .$$

This single-spin asymmetry may be measured at the future GSI $p\overline{p}$ experiment and the up-graded DAFNE experiment.

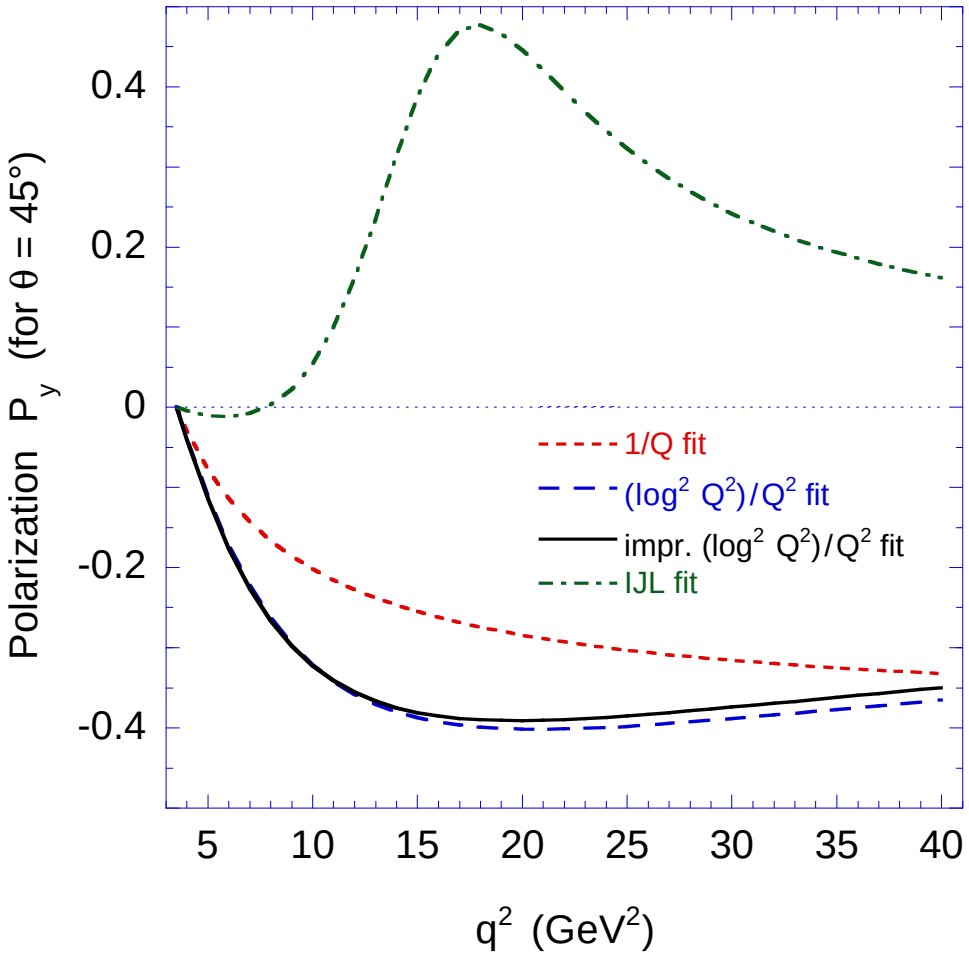

Predicted polarization $\mathcal{P}_y$ in the timelike region for selected form factor fits described in BCHH (Brodsky, Carlson, Hiller, Hwang, 2004). The plot is for $\theta = 45°$. The four curves are for an $F_2/F_1 \propto 1/Q$ fit, using BCHH 1; the $(\log^2 Q^2)/Q^2$ fit of Belitsky et al.; an improved $(\log^2 Q^2)/Q^2$ fit, BCHH 2; and a fit from Iachello et al.

Single-Spin Asymmetry in $ep^{\uparrow} \to e\pi X$

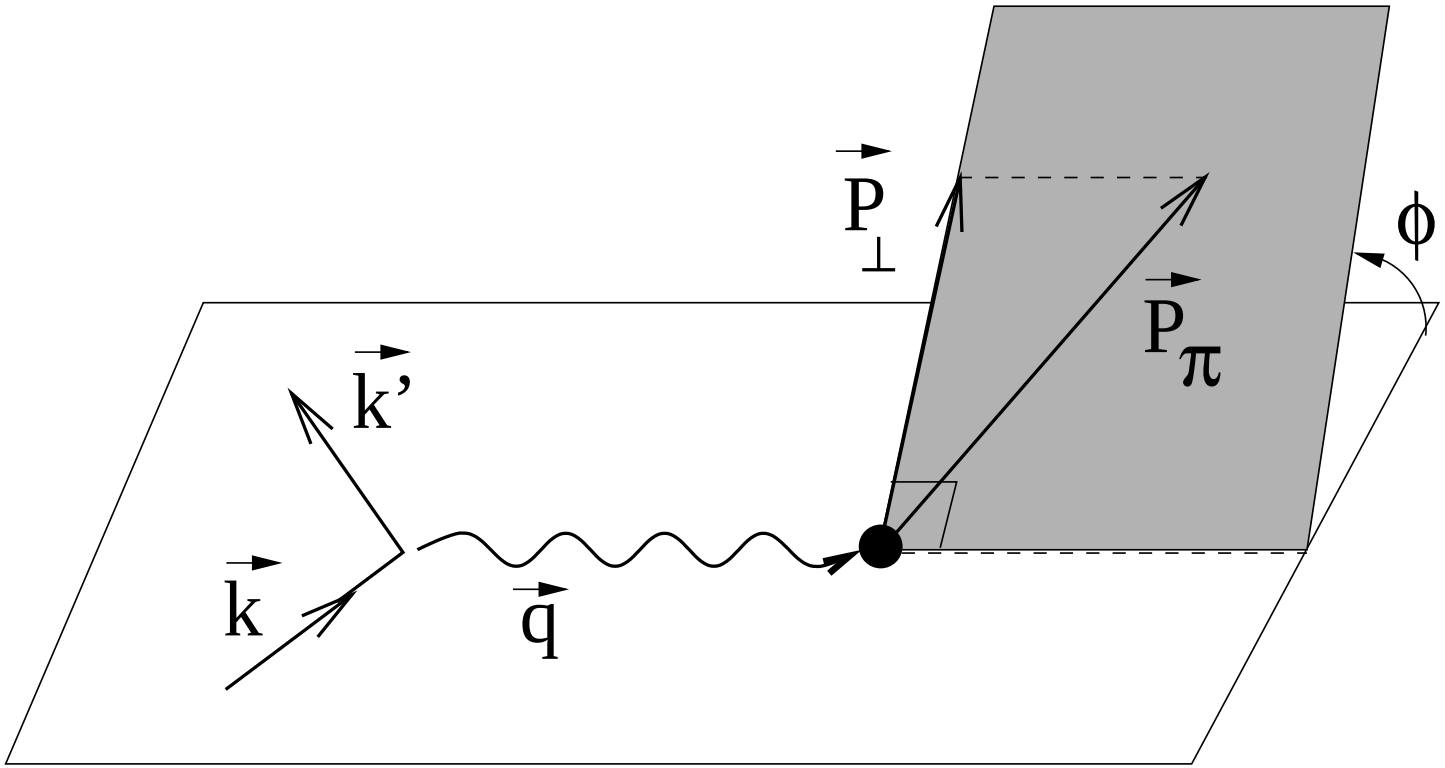

Kinematic planes for pion production in semi-inclusive deep-inelastic scattering.

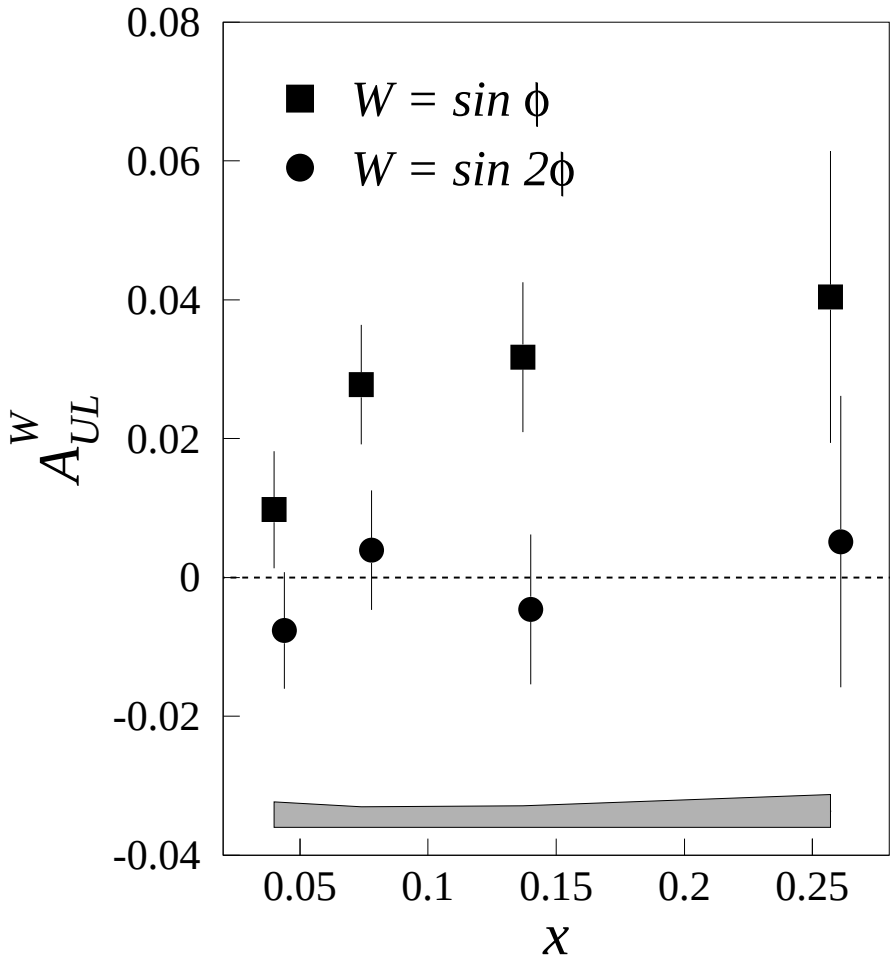

Hermes (DESY) Result, 2000. Target-spin analyzing powers for π^+: $A_{UL}^{\sin\phi}$ (squares) and $A_{UL}^{\sin 2\phi}$ (circles) as a function of Bjorken x. Error bars show the statistical uncertainty and the band represents the systematic uncertainties for $A_{UL}^{\sin\phi}$.

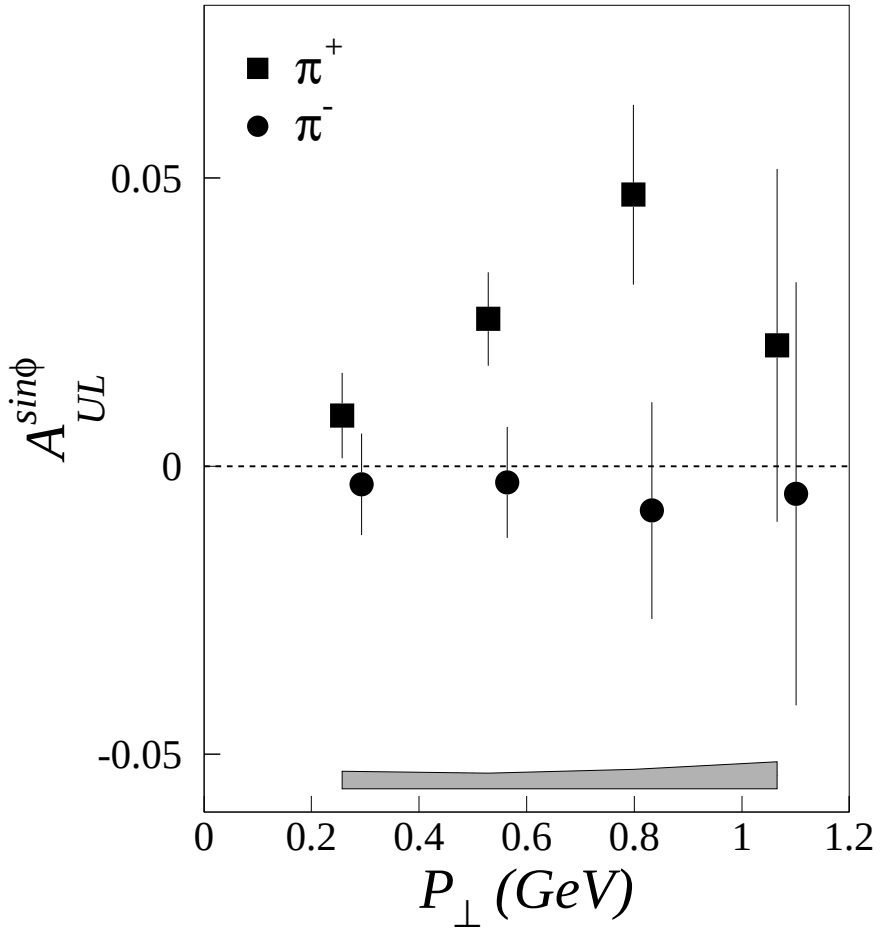

Hermes (DESY) Result, 2000. Target-spin analyzing powers in the $\sin\phi$ moment as a function of transverse momentum, for π^+ (squares) and π^- (circles). Error bars show the statistical uncertainties and the band represents the systematic uncertainties.

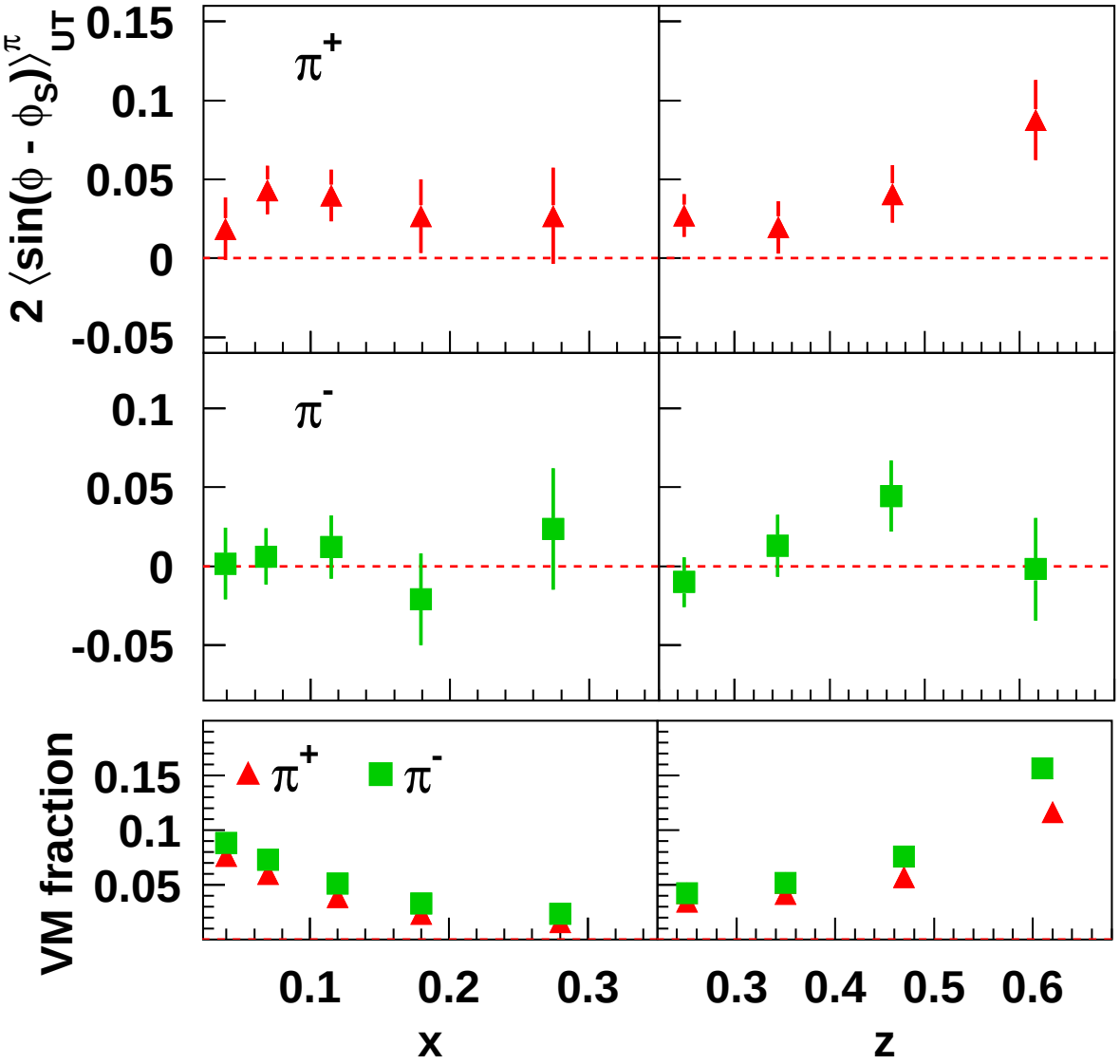

Hermes (DESY) Result, 2005. Sivers moments for charged pions as a function of x and z. The error bars represent the statistical uncertainties. The lower panel shows the relative contributions to the data from simulated exclusive vector meson production.

Single-Spin Asymmetry in $ep^{\uparrow} \rightarrow e\pi X$

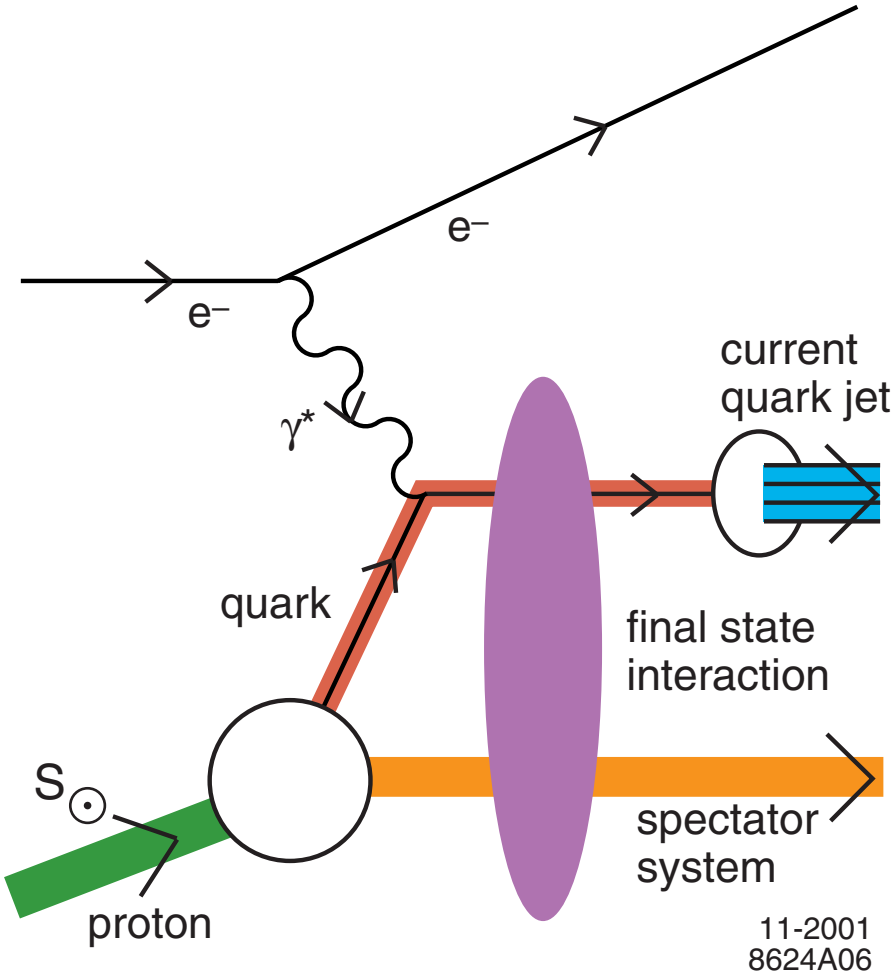

Explicit Model Calculations

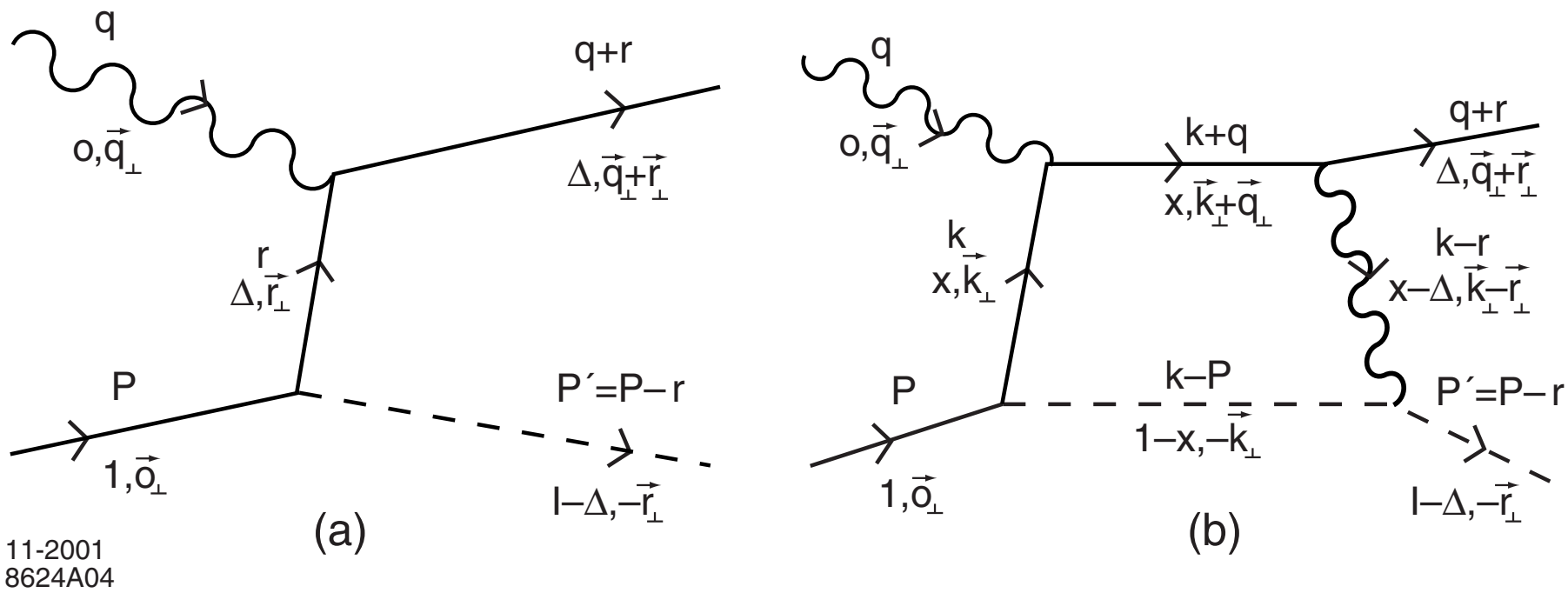

(a) Tree level diagram and (b) diagram with fanal state interaction. (Brodsky, Hwang, Schmidt, 2002)

The contributing amplitudes for $\gamma^* p \to q(qq)_0$ have the following structure through one loop order:

$$
\begin{aligned}
A(\Uparrow\to\uparrow) &= (M+\frac{m}{\Delta})\, C\, (h + i\frac{e_1 e_2}{8\pi} g_1) \\
A(\Downarrow\to\uparrow) &= (\frac{+r^1 - ir^2}{\Delta})\; C\, (h + i\frac{e_1 e_2}{8\pi} g_2) \\
A(\Uparrow\to\downarrow) &= (\frac{-r^1 - ir^2}{\Delta})\; C\, (h + i\frac{e_1 e_2}{8\pi} g_2) \\
A(\Downarrow\to\downarrow) &= (M+\frac{m}{\Delta})\, C\, (h + i\frac{e_1 e_2}{8\pi} g_1)\ ,
\end{aligned}
$$

where

$$
\begin{aligned}
C &= -\, g\, e_1\, P^+ \sqrt{\Delta}\, 2\, \Delta\, (1-\Delta) \\
h &= \frac{1}{\vec{r}_\perp^{\,2} + \Delta(1-\Delta)(-M^2 + \frac{m^2}{\Delta} + \frac{\lambda^2}{1-\Delta})}\ .
\end{aligned}
$$

$$g_1 = \int_0^1 d\alpha$$

$$\times \quad \frac{1}{\alpha(1-\alpha)\vec{r}_\perp^{\,2} + \alpha\lambda_g^2 + (1-\alpha)\Delta(1-\Delta)(-M^2 + \frac{m^2}{\Delta} + \frac{\lambda^2}{1-\Delta})}$$

$$g_2 = \int_0^1 d\alpha$$

$$\times \quad \frac{\alpha}{\alpha(1-\alpha)\vec{r}_\perp^{\,2} + \alpha\lambda_g^2 + (1-\alpha)\Delta(1-\Delta)(-M^2 + \frac{m^2}{\Delta} + \frac{\lambda^2}{1-\Delta})} \; .$$

The rescattering phases $e^{i\chi_i}\ i = 1, 2$ with $\chi_i = \tan^{-1}(\frac{e_1 e_2}{8\pi}\frac{g_i}{h})$ are thus distinct for the spin-parallel and spin-antiparallel amplitudes. g_1 and g_2 are both infrared divergent, however, the difference $(g_1 - g_2)$ is infrared finite. SSA is proportional to $(g_1 - g_2)$.

The single-spin asymmetry transverse to the production plane is given by

$$\begin{aligned}
\mathcal{P}_y &= \frac{e_1 e_2}{8\pi} \frac{2\left(\Delta M + m\right) r^1}{\left[\left(\Delta M + m\right)^2 + \vec{r}_\perp^{\,2}\right]} \\
&\times \left[\vec{r}_\perp^{\,2} + \Delta(1-\Delta)(-M^2 + \frac{m^2}{\Delta} + \frac{\lambda^2}{1-\Delta})\right] \\
&\times \frac{1}{\vec{r}_\perp^{\,2}} \ln \frac{\vec{r}_\perp^{\,2} + \Delta(1-\Delta)(-M^2 + \frac{m^2}{\Delta} + \frac{\lambda^2}{1-\Delta})}{\Delta(1-\Delta)(-M^2 + \frac{m^2}{\Delta} + \frac{\lambda^2}{1-\Delta})} \,.
\end{aligned}$$

The linear factor of $r^1 = r^x$ reflects the fact that the single spin asymmetry is proportional to $\vec{S}_p \cdot \vec{q} \times \vec{r}$ where $\vec{q} \sim -\nu\hat{z}$ and $\vec{S}_p = \pm\hat{y}$. Here $\Delta = x_{bj}$.

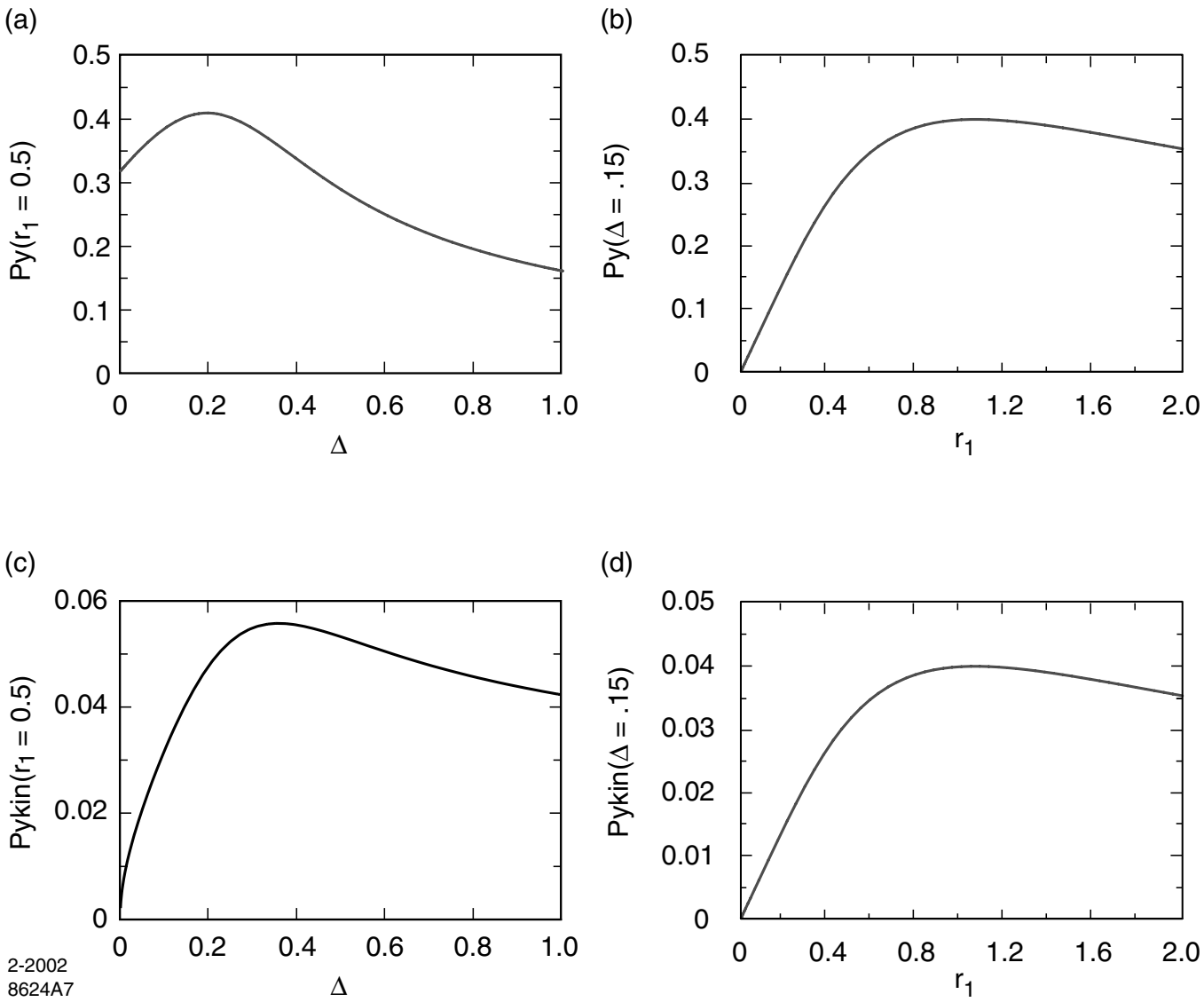

Model predictions for the single spin asymmetry of the proton in electroproduction resulting from gluon exchange in the final state as a function of $\Delta = x_{bj}$ and quark transverse momentum $r_\perp$. The parameters are given in the text.

Final-state interactions from gluon exchange lead to single spin asymmetries in DIS at leading twist in perturbative QCD; *i.e.*, the rescattering corrections are not power-law suppressed at large photon virtuality Q^2 at fixed x_{bj}.

The existence of such single-spin asymmetries requires a phase difference between two amplitudes coupling the proton target with $J_p^z = \pm\frac{1}{2}$ to the same final-state.

Time-odd (naive) distribution functions

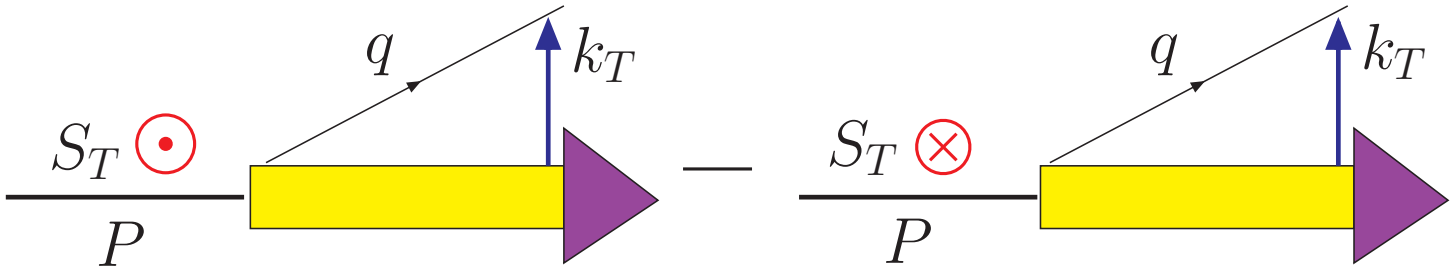

Sivers distribution function $f_{1T}^{\perp}$.

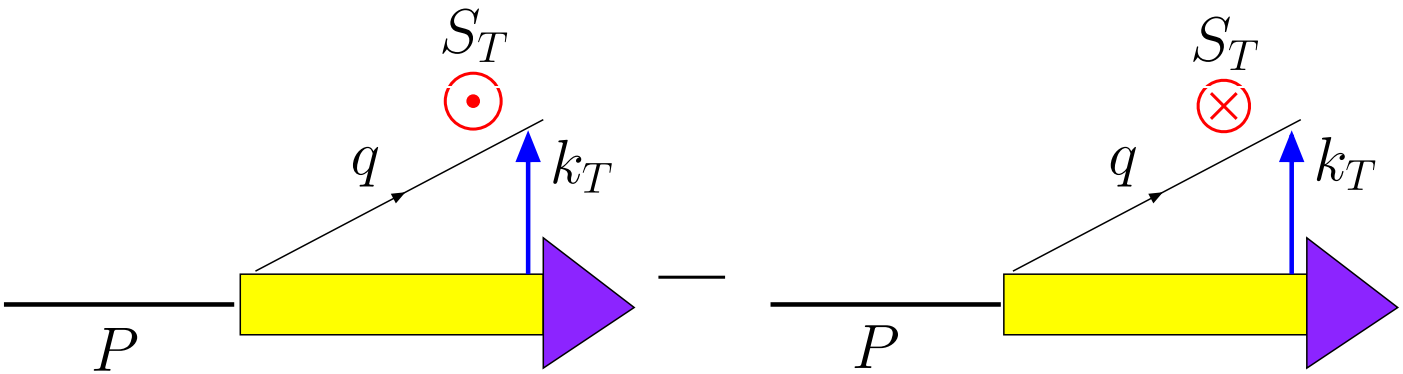

Boer-Mulders distribution function $h_1^{\perp}$.

Sivers and Boer-Mulders DF

$$\Phi(x,\vec{k}_\perp : P,S) = \frac{M}{2P^+}\Big[\, f_1(x,\vec{k}_\perp)\,\frac{\gamma\cdot P}{M} + f_{1T}^\perp(x,\vec{k}_\perp)\,\epsilon_{\mu\nu\rho\sigma}\frac{\gamma^\mu P^\nu k_\perp^\rho S_T^\sigma}{M^2} + h_1^\perp(x,\vec{k}_\perp)\,\frac{\sigma_{\mu\nu}k_\perp^\mu P^\nu}{M^2} + \cdots \Big] .$$

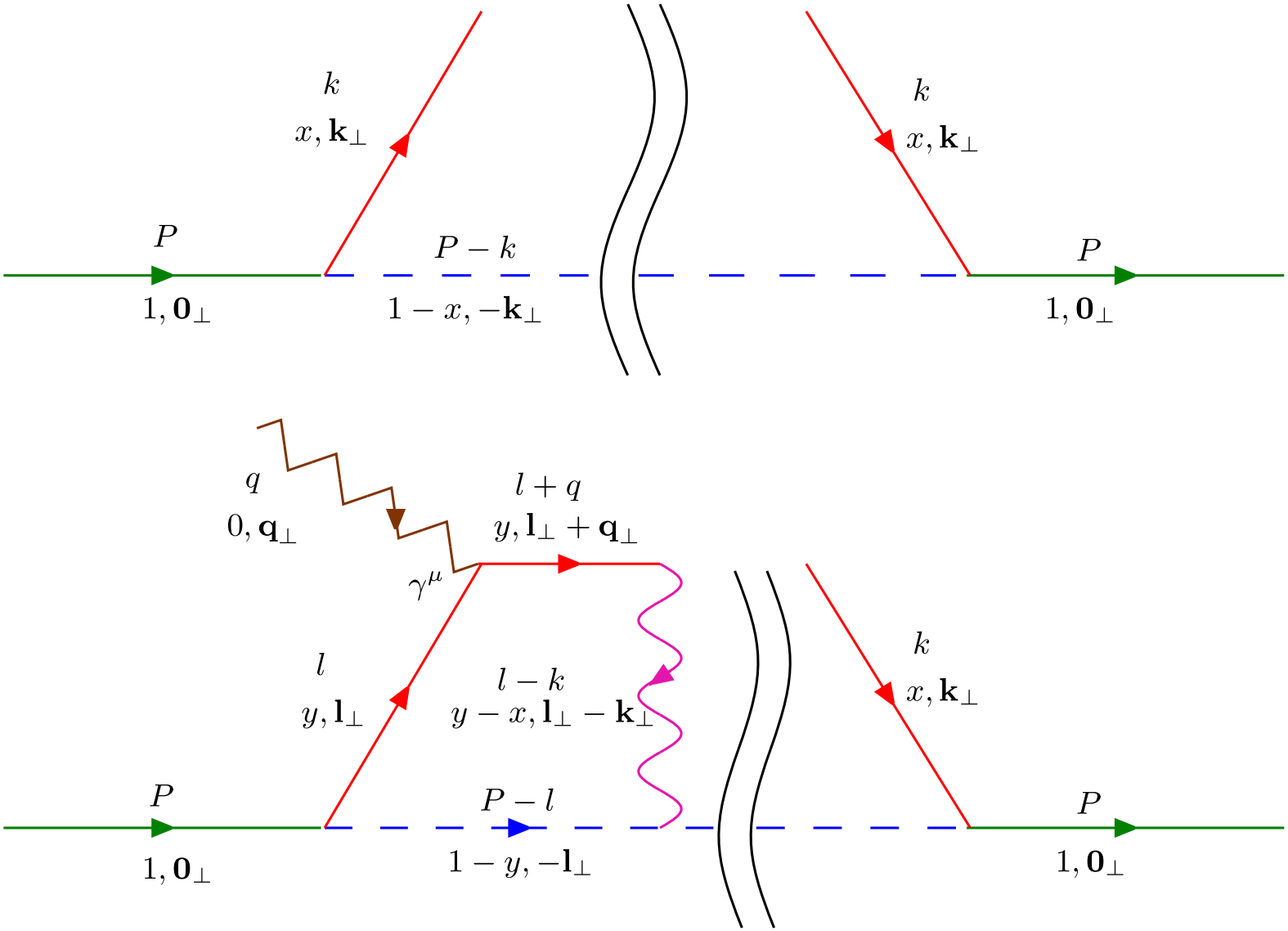

Diquark model diagrams for f_1, $f_{1T}^\perp$ and $h_1^\perp$.

Polarized Drell-Yan Process

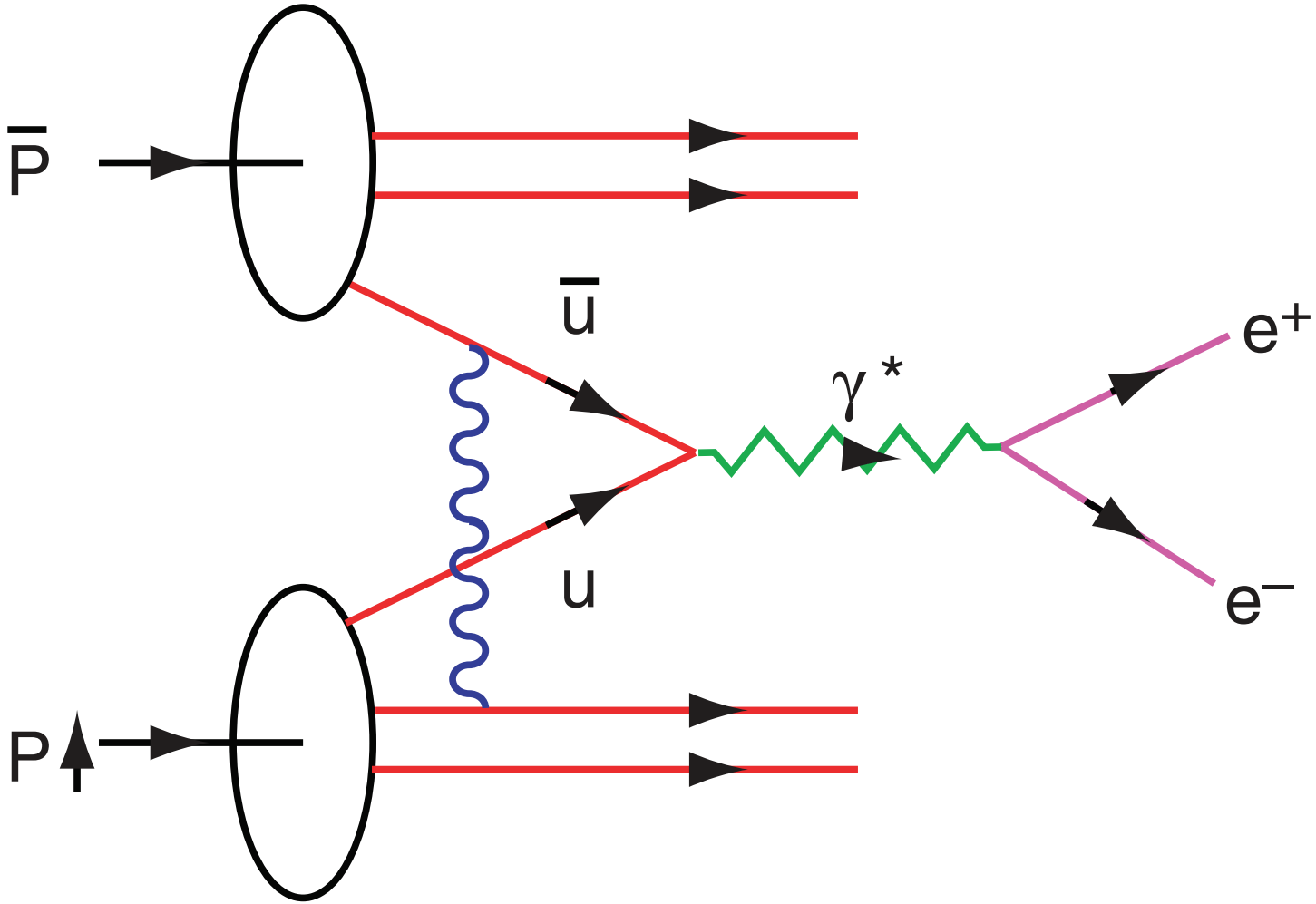

The initial-state interaction in the Drell-Yan process.

Violating naive universality of parton densities:

$$f_{1T}^{\perp}(x, k_T, \zeta)|_{\rm DIS} = -f_{1T}^{\perp}(x, k_T, \zeta)|_{\rm DY}.$$

Collins (2002), Brodsky, Hwang, Schmidt (2002)

This can be checked at COMPASS and RHIC.

Unpolarized Drell-Yan Process

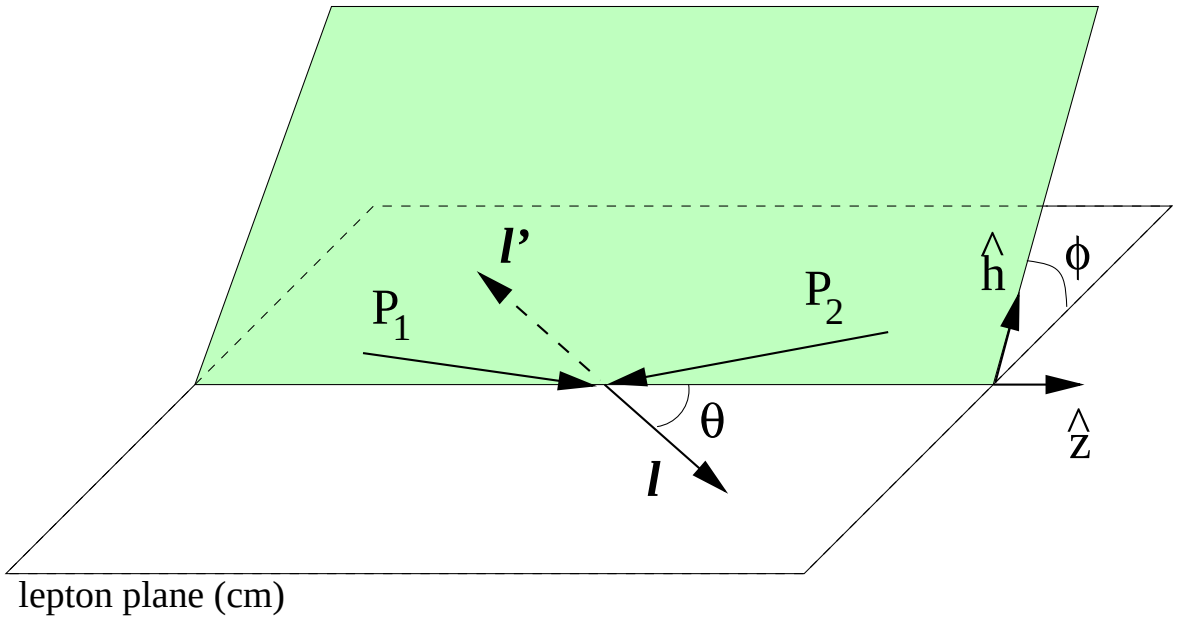

Kinematics of the Drell-Yan process in the lepton center of mass frame.

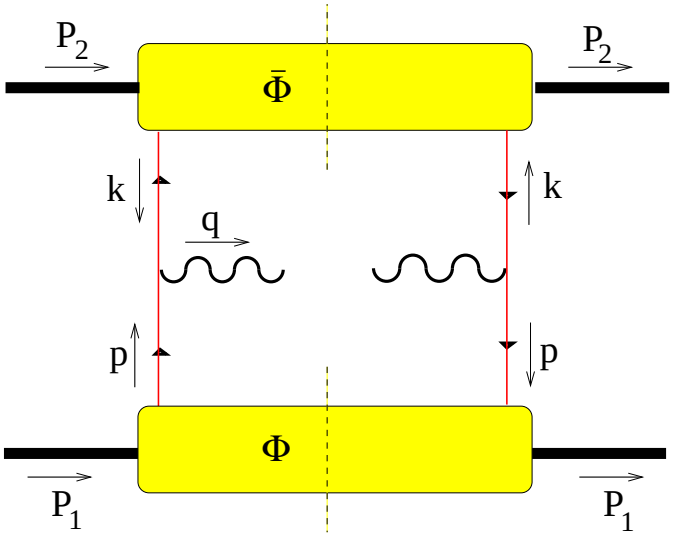

The leading order contribution to the Drell-Yan process.

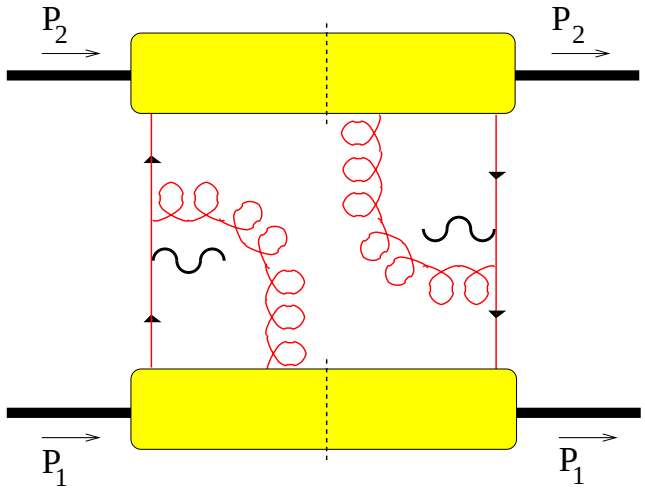

The initial-state interaction contribution to the Drell-Yan process.

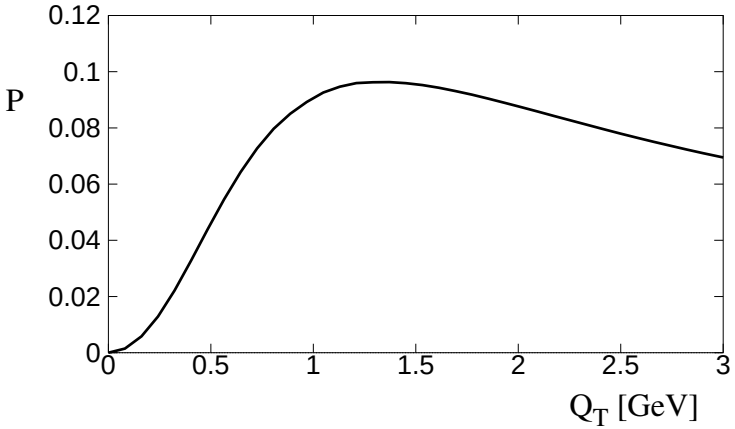

Numerical result for P. $\nu \approx 3P$.

$$\frac{1}{\sigma}\frac{d\sigma}{d\Omega} = \frac{3}{4\pi}\frac{1}{\lambda+3}\left(1+\lambda\cos^2\theta+\mu\sin^2\theta\cos\phi+\frac{\nu}{2}\sin^2\theta\cos 2\phi\right).$$

The Lam-Tung relation $1-\lambda-2\nu=0$ is violated by this mechanism of $h_1^\perp \times \overline{h}_1^\perp$ from the initial state interactions, whereas this relation is expected to hold at order α_s and the relation is hardly modified by next-to-leading order (α_s^2) perturbative QCD corrections.

Boer (1999), Boer, Brodsky, Hwang (2003)

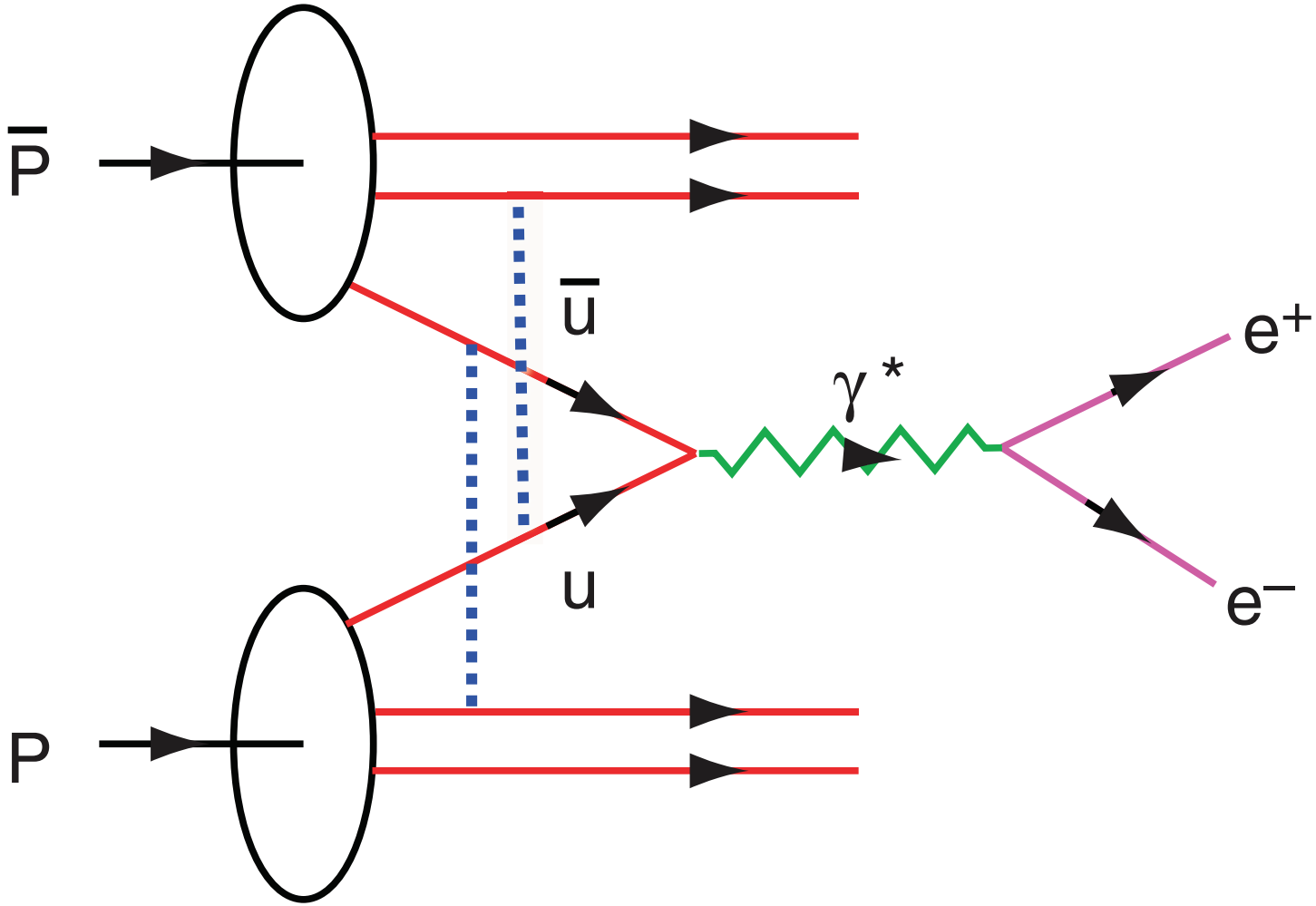

$$h_1^\perp \times \overline{h}_1^\perp$$

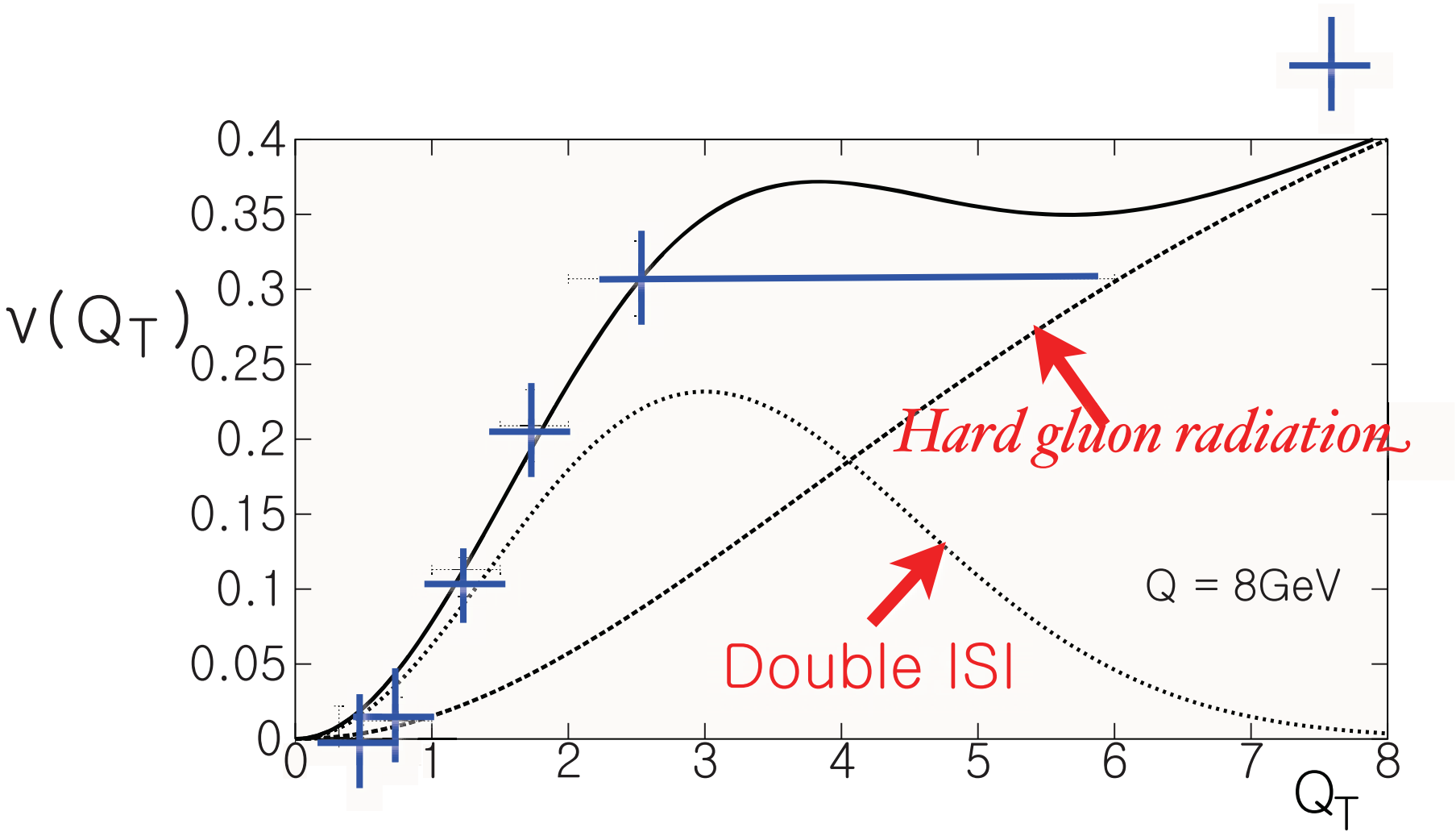
$v(Q_T)$
0.4
0.35
0.3
0.25
0.2
0.15
0.1
0.05
0
0
1
2
3
4
5
6
7
8
Q_T
Hard gluon radiation
Double ISI
Q = 8GeV

Λ Polarization at LHC

Boer, Bomhof, Hwang, Mulders, 2008

Feynman x_F is small in ALICE.
So, no polarization for

$$P + P \to \Lambda^{\uparrow} + X.$$

Instead, consider

$$P + P \to (\Lambda^{\uparrow}\mathrm{jet}) + \mathrm{jet} + X.$$

Then, in the jet-jet center of mass frame,

$$\epsilon_{\mu\nu\lambda\rho} k_1^{\mu} k_2^{\nu} k_3^{\lambda} S^{\rho} \to \vec{S}_{\Lambda} \cdot (\vec{K}_{\mathrm{jet}} \times \vec{K}_{\Lambda}).$$

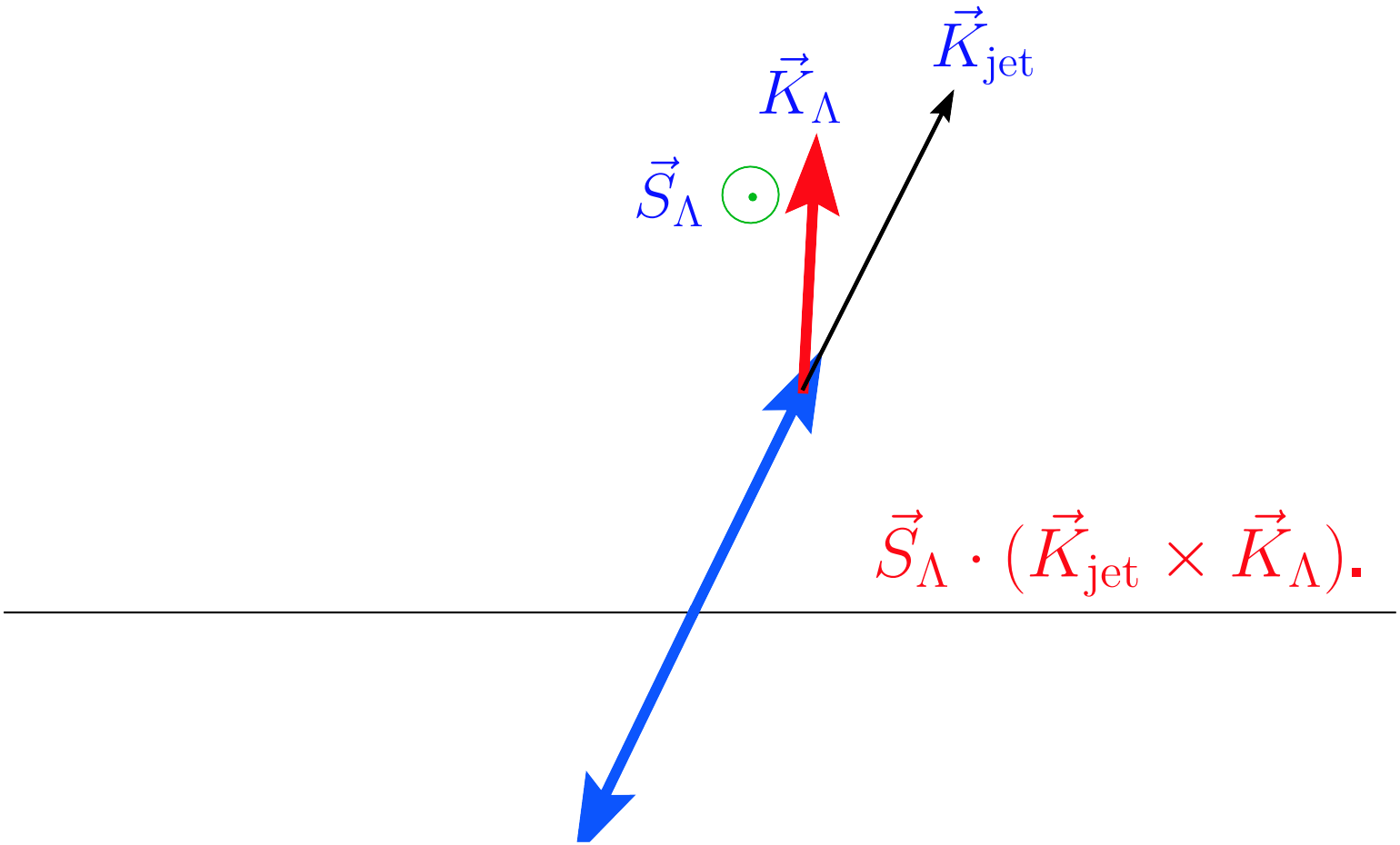

In the jet-jet center of mass frame.

Summary

Final-state interactions from gluon exchange lead to single spin asymmetries in SIDIS at leading twist in perturbative QCD; *i.e.*, the rescattering corrections are not power-law suppressed at large photon virtuality Q^2 at fixed x_{bj}.

In SIDIS and polarized Drell-Yan processes, violation of naive universality of parton densities:

$$f_{1T}^{\perp}(x, k_T, \zeta)|_{\rm DIS} = -f_{1T}^{\perp}(x, k_T, \zeta)|_{\rm DY}.$$

In unpolarized Drell-Yan process, $\cos 2\phi$ angular distribution of the lepton pair is induced by $h_1^{\perp} \times \overline{h}_1^{\perp}$ from the initial-state interactions.